DOI: 10.23968/2500-0055-2024-9-1-71-78

# COMPARATIVE BUCKLING ANALYSIS OF CONCRETE AND EXPANDED POLYSTYRENE DOME SHELLS

Habte Yohannes Damir[1,2]*, Marina Rynkovskaya[1], Issaias Anday Sereke[1,2]

[1] Peoples' Friendship University of Russia named after Patrice Lumumba (RUDN University), Moscow, Russia
[2] Mai Nefhi College of Engineering and Technology, Asmara, Eritrea

*Corresponding author's e-mail: habte88eng@gmail.com

**Abstract**

**Introduction:** Various studies have been conducted to analyze the buckling behavior of concrete spherical shells. Nonetheless, no research is available that would investigate the buckling behavior of EPS (expanded polystyrene) shells. EPS has a very low self-weight compared to concrete. **The purpose of the study** is to investigate the comparative buckling characteristics of concrete and EPS shells. The respective self-weight and live load of 1.5 kN/m$^2$ were considered. **The methods** used are Linear buckling analysis (LBA) and geometrically nonlinear buckling analysis (GNA) of sample domes with and without imperfections performed using Abaqus software. **The results** of the comparative analyses show that the critical buckling pressure of EPS and concrete spherical shells of the same geometry was found to be 122,634 N/m$^2$ and 5560 N/m$^2$, respectively. The ratio of the critical buckling pressure to the practical ultimate (dead load + live load) loading of concrete is 23.2, while for EPS, it is 2.22. Moreover, increasing the thickness of EPS from 100 to 200 mm increased the critical buckling pressure factor by 15.4 times. The maximum loading displacement of EPS (15.6 mm) was times less than the displacement caused by the buckling pressure. This finding demonstrates the feasibility of constructing EPS shells, with further research on the optimum geometry and construction mechanism.

**Keywords:** shells, buckling, dome, concrete, EPS.

## Introduction

*Shell structures*

In general, shell structures are defined as spatially curved surface structures that support externally applied loads (Farshad, 1992). Accordingly, shells can be described as structures with a small thickness compared to their other dimensions, which can be used to cover large spans by developing in-plane stresses under the actions of membrane forces (Ter Maten et al., 2013). Adriaenssens et al. (2014) defined shell structures as “constructed systems described by three-dimensional curved surfaces, in which one dimension is significantly smaller compared to the other two. They are form-passive and resist external loads predominantly through membrane stresses”. Shells are structures with the most efficient structural elements, found in both nature and technological designs. The generation of shell surfaces, from a theoretical perspective, could be considered the most effective construction method (Huijben et al., 2011). The use of new materials in thin pavilions, experimental structures, and shells promotes the development of future architecture (Jovanovic et al., 2017).

To achieve effective design of shell structures, it is important to optimize the geometric shape as well as the material usage to make the structure as light as possible. In the context of optimizing material use, the practical utilization of various materials such as concrete, steel, masonry blocks, EPS, and others can be considered for optimum alternative selection. When it comes to concrete structures, their self-weight is the main component of the overall structural load. Concrete shell structures have been widely used since the 1930s (Huijben et al., 2011). Concrete is a widely used structural construction material, and EPS is also well known for its implementation in various structural sectors as a filler and insulation, often used to cover slabs and stairs. It is known as a light-weight material due to its relatively low density. Ibrahim et al. (2013) advocate that their study confirms that the compressive strength of EPS with an appropriate thickness was found to be adequate to support dead and live loads. Furthermore, the study by Khalaj et al. (2020) demonstrates that the elastic modulus of EPS increases with an increase in EPS density. For a better comparative display, the structural properties of concrete and EPS are summarized below in Table 1.

In any structural analysis, the stability of shell structures is of primary importance. The behavior of the material structure should be determined from the ultimate buckling loads and load-displacement relations (Ellobody et al., 2014). The design of a thin shell is generally more governed by buckling stability requirements, rather than just by the material strength and characteristics.

This paper examines the critical buckling loads that can be induced in concrete and EPS shells in comparison to their characteristic strength, which

determines the maximum deformation of a given geometry.

*Buckling analysis of spherical shells*

The critical buckling load pressure for the stability analysis of shells of revolution can be computed using the governing equations given below (Mekjavić, 2011). These equations are derived from the equation for computing the buckling load of a full sphere, which is used to approximate the buckling load for a dome shell.

$$q_{cr} = \frac{2E}{\sqrt{3\left(1-v^2\right)}}\left(\frac{t}{r}\right)^2, \quad (1)$$

where: $q_{cr}$ (in MPa) is critical buckling pressure, with $E$, v, $t$, and $r$ being the modulus of elasticity (GPa), Poisson's ratio, shell thickness (m), and shell radius (m), respectively.

The corresponding critical stress ($\sigma_{cr}$) can be determined as follows:

$$\sigma_{cr} = \frac{q_{cr}r}{2t} = \frac{Et}{r\sqrt{3\left(1-v^2\right)}}. \quad (2)$$

In this study, a comparative analysis was performed using nonlinear finite element analysis with Abaqus software. All structural responses, such as deformations, stresses, and buckling, were analyzed. To investigate the displacement of the load against the maximum magnitudes, a manual computation was performed using Eqs. 1 and 3 (see details in *Results of Loading Displacements*). The applied load pressure includes the self-weight and an area live load of 1.5 kN/m$^2$ normal to the surface.

**Materials and methods**

Concrete in general is made from mixtures of cement, sand, aggregates, and water in a designed proportion (Gagg, 2014). Normal concrete has a unit weight of 22–25 kN/m$^3$. The high density of concrete is the main factor contributing to the self-weight loading in load combination cases. As can be noted from Table 1, concrete has a compressive strength that is about 10 times higher than its tensile strength. This demonstrates that concrete is fundamentally brittle and becomes stronger when compressed. In contrast, due to its low tensile strength, it is prone to failure from shearing and/or tensile forces. In this study, the randomly selected concrete has the following properties:

$\gamma_c$ = 24 kN/m$^3$ $E_c$ = 30 GPa Poison's ratio: 0.2

where: $\gamma_c$ and $E_c$ are the unit weight and modulus of elasticity of the concrete used for the analyses.

EPS is a light-weight cellular polymeric material used in various areas of civil engineering (Khalaj et al., 2017, 2020; Ni et al., 2020; Ramli Sulong et al., 2019; Vilau and Dudescu, 2020). The individual granular components of EPS can be found in varying fine sizes and shapes, including circular, hexagonal, octagonal, and others. EPS is used in various construction applications to withstand different loading stresses. According to Table 1, it has a relatively low unit weight ranging from 0.12 to 0.35 kN/m$^3$, which is approximately 100 times lower than that of concrete. Similarly, EPS has very low compressive strength characteristics of 0.04–10.9 MPa. Nonetheless, its tensile strength is about 10 times higher than that of concrete. Another important factor is the modulus of elasticity of EPS, which is on average 1.32 GPa, almost 30 times less than that of concrete. With all these different values, it is important to investigate the feasibility of using EPS material in shell structures. Furthermore, concrete and EPS materials can be mixed to achieve the desired characteristics. The experimental study by Saheed et al. (2020) demonstrates that a composite EPS-concrete slab structure has the potential to be a construction material with combined density and strength benefits.

For this reason, the authors of this paper searched for research articles related to the analysis of EPS shell structures in Google Scholar, ResearchGate, and Google search engines. Surprisingly, no single article was found that would provide detailed structural analysis regarding the material strength and stability requirements of EPS shells. The only paper related to EPS shell structures found from

Table 1. **Varying material properties of concrete and EPS**

| No. | Symbol | Description | Unit | Concrete | EPS |
|---|---|---|---|---|---|
| 1. | γ | Unit weight | kN/m$^3$ | 22–25 | 0.12–0.35 |
| 2. | $f_c$ | Compressive strength | MPa | 20–40 | 0.04–10.9 |
| 3 | $f_t$ | Tensile strength | MPa | 2–5 | 47–51 |
| 4. | $f_b$ | Flexural strength | MPa | 0.864 –1.207 | 0.075–3 |
| 5. | V | Shear strength | MPa | 6–17 | 0.124–0.3 |
| 6. | E | Modulus of elasticity | MPa | 14,000–41,000 | 6.5–2650 |
| 7. | μ | Permeability | cm/s | $10^{-10}$ | 0.5–3.5 |
| 8. | α | Coefficient of thermal expansion | C1 | $10^{-5}$ | 63–80 |
| 9. | v | Poisson's ratio | - | 0.2–0.21 | 0.05–0.5 |
| 10 | k | Thermal conductivity | W/m·k | | 0.027–0.045 |

a Google search was the paper by Jovanovic et al. (2017). In that paper, the experimental model (Fig. 1) illustrates the tessellation and robotic form generation of a parabolic shell revolution, but does not include the structural analysis.

This paper is aimed at investigating the structural and kinematic responses of EPS shell forms in comparison to concrete shells of similar geometry. Spherical dome shapes were developed and analyzed for EPS and concrete materials. The two models were analyzed for the same geometric shape dimensions and thickness. The EPS parameters of unit weight ($\gamma_{eps}$), modulus of elasticity ($E_{eps}$), and Poisson's ratio (v) used in the calculations are as mentioned below:

$\gamma_{eps}$ = 0.24 kN/m$^3$ $E_{eps}$ = 1.32 GPA

Poison's ratio, v = 0.275

The availability of advanced computer programming tools made it possible to analyze the nonlinear behavior of shells (Eisenbach, 2017). To optimize the structural behavior, several models were developed by making geometric and size modifications. The ideal numerical models of the two materials were analyzed. Moreover, it is important to develop a template model that can be consistently used throughout the process of form generation and structural analysis, to evaluate stability and deformations using general finite element analysis. The evaluation of kinematic indeterminacy and the analysis of large deformations in concrete and EPS shells were eventually investigated.

*Linear buckling analysis*

Eigenvalue linear buckling analysis is commonly used to determine the critical buckling load of a structure (Novoselac et al., 2012). Eigenvalue buckling analysis is described as an analysis of linear buckling, where the structures are considered to be elastic and without imperfections. Nevertheless, no structure is purely elastic in every situation and it cannot be free of any imperfections due to discrepancies in geometries, material properties, and workmanship (Imran et al., 2020). Performing nonlinear buckling analysis along with linear analysis is important for creating more accurate models (LUSAS, 2017).

*Geometrically nonlinear buckling analysis*

Geometrically nonlinear analysis is also referred to as load-displacement nonlinear geometry analysis (Ellobody et al., 2014). When geometric nonlinearity is considered, a significant deviation of deflection from the linear effect of loading exists (Semenov, 2016). As discussed in the previous section, GNA follows the initial conditions of stress analysis or linear eigenvalue buckling. Moreover, spherical shells are extremely susceptible to nonlinear buckling conditions when subjected to external pressure loads (Hutchinson and Thompson, 2017). In this paper, the effects of geometric nonlinearity and imperfections on the behavior of the selected material properties of concrete and EPS spherical shells are examined. Nonlinear buckling analyses were carried out in Abaqus software. As a result, the conditions for the ultimate load pressure and load displacement were determined for the given shell geometries and material properties. For both materials under consideration, an ideal spherical dome shell with the same geometric details for both materials and a thickness of 0.1 m is shown in Fig. 2.

**Results and discussion**

Linear buckling analysis models of the two materials were run in Abaqus software. The maximum buckling pressure was determined based on the respective moduli of elasticity of concrete (30 GPa) and EPS (1.32 GPa). Accordingly, the eigenvalues of the concrete and EPS domes generated from the LBA were found to be 0.39 MPa and 0.018 MPa, respectively. Furthermore, the maximum buckling pressure determined by the GNA was found to be 0.122 MPa (concrete) and 0.005560 MPa (EPS).

*LBA results*

According to the LBA, the maximum displacements in the concrete and EPS models under the first eigenvalue pressure were found to be 1 m and 1.364 m, respectively. These values exist for plain, unreinforced concrete and EPS shells with a thickness of 0.1 m and a span of 48 m, under the eigenvalue pressure of 0.395 MPa and 0.018 MPa, respectively. These LBA loadings are approximately 70 and 7.4 times the ultimate imposed loadings listed in Table 2. These displacements are significantly

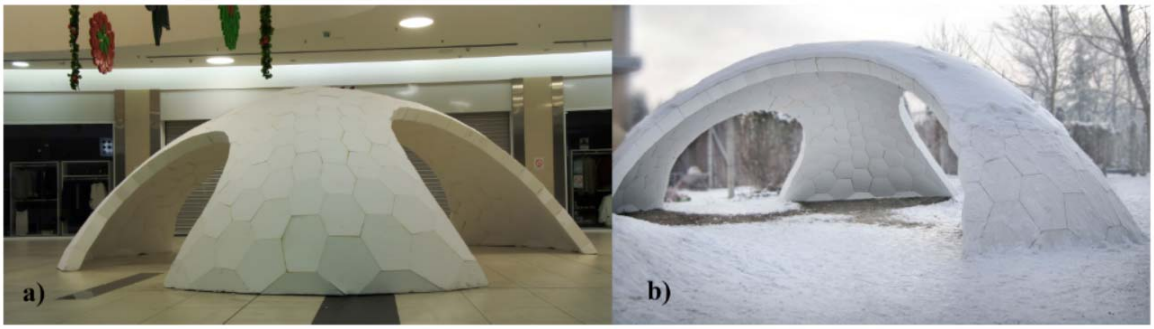


Fig. 1. Experimental EPS shell structure (Jovanovic et al., 2017)

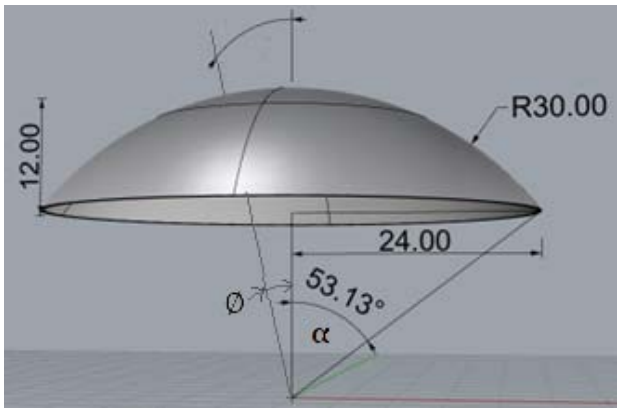


Fig. 2. Geometric details of the dome-shaped shell under analysis

reduced when the models are analyzed in GNA, as discussed in the following sections. Moreover, in real-world construction, using appropriate thicknesses and actual loads (which are much smaller than LBA loads) and considering reinforcement can result in feasible deformations. The linear buckling analysis is computed taking into account the respective values of modulus of elasticity and Poisson's ratio. The maximum deflection in EPS demonstrates a 36% higher value compared to concrete, as the deflection computation is not linearly proportional to the values of E and eigenvalue taken.

*GNA results*

The geometric nonlinear analyses were performed without and with imperfection considerations, as shown in Figs. 3–5, respectively. Shell structures are known to be very sensitive to loading and geometric imperfections. Generally, spherical domes are classified as either shallow, deep, or complete based on the central vertical angle (Wagner et al., 2020). In this study, a half central angle of 53° was considered. Furthermore, the behavior of spherical domes towards imperfections is governed by the angles taken from the edges (Tomas et al., 2009). It is stated that for spherical shells loaded by uniform pressure, critical loads are highly sensitive to initial geometric imperfections (Bushnell, 1981). Furthermore, the paper argues that open cap spherical (dome) shells are likely to exhibit non-symmetric buckling modes depending on their shallowness. Considering the effects of imperfection sensitivity in concrete domes, it is recommended to apply a reduction factor ranging from 0.05 to 0.1 to the theoretical buckling load (Farshad, 1992). Tomas et al. (2009) argue that imperfections in concrete domes are unavoidable, as material homogeneity is affected by creep, plasticity, and cracking. They emphasize that for homogeneous elastic materials, a value of 1 is taken if the shell is sensitive to imperfections; otherwise, a value less than 1 is used. Considering an average value from this range, such as 0.075, an imperfection amplitude is applied in ABAQUS.

The results of the GNA performed without imperfections are displayed, showing maximum displacement magnitudes of 0.090 m for concrete and 0.289 m for EPS, as depicted in Figs. 3 and 4, respectively. Similarly, simulations with imperfections exhibit maximum displacements of 0.456 m for concrete and 0.643 m for EPS, as shown in Fig. 5. The displacement deviation induced by imperfections appears to be 4.5 times greater in concrete and 2.22 times greater in EPS. This result aligns with the logic that EPS has a larger Poisson's ratio and elasticity.

Despite the loading being symmetrical, applying the first eigen mode as an imperfection test with an imperfection amplitude of 0.075 causes the dome to exhibit non-symmetrical behavior.

*Results of loading displacements*

The displacement resulting from each imposed ultimate load was calculated using both the analytical formula shown in Eq. (3) and numerical analysis conducted with Abaqus software.

The comprehensive formula (w) is used to determine the deformation field in a spherical shell as follows:

$$W_{\varnothing} = \frac{R^2 q}{Et} \times \left[ \begin{array}{c} \left( \cos\varnothing - \frac{1}{1+\cos\varnothing} \right) + \\ (1+v)\cos\varnothing \left[ \ln(1+\cos\varnothing) - \right. \\ \left. -\ln(1+\cos\alpha) + \frac{1}{1+\cos\alpha} - \frac{1}{1+\cos\varnothing} \right] \end{array} \right], \quad (3)$$

where: Φ is the meridian angle from the central axis to the points of consideration and α is the overall meridional angle of the dome. In this study, the dome radius and meridian angles are taken as R = 30 m; Φ = 0; α = 53.130. As shown in Fig. 2, the value of α is the half central angle of the dome shell and Φ = 0 represents the location of the top crest of the dome.

The displacement resulting from the loading (self-weight dead load + 1.5 KN/m$^2$ live load) was calculated using Eq. (3) for both the concrete and EPS shells of the same geometry, as shown in Table 2. The loads are factored into the ultimate load combination using the American Concrete Institute (ACI) loading code [1.2x Dead Load (DL) + 1.6x Live Load (LL)].

The results in Table 2 show that for a thickness of 100 mm in concrete and EPS domes, the maximum displacements are 1.45 mm and 15.6 mm, respectively, under their respective self-weight and 1.5 KN/m$^2$ live load. These results are more accurate and stable compared to the magnitude of maximum displacements computed for buckling analysis. Furthermore, in Tables 3 and 4, the

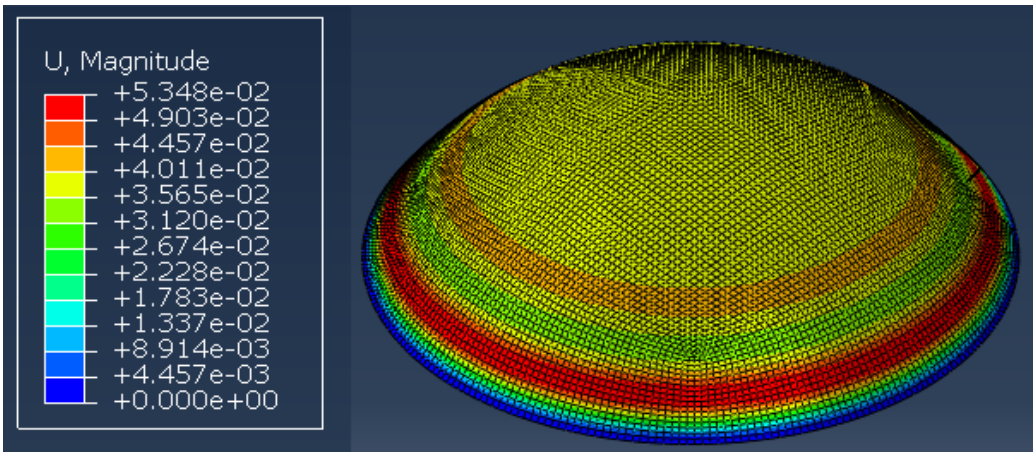


Fig. 3. Deformed shape of concrete with maximum displacement after GNA analysis without imperfections

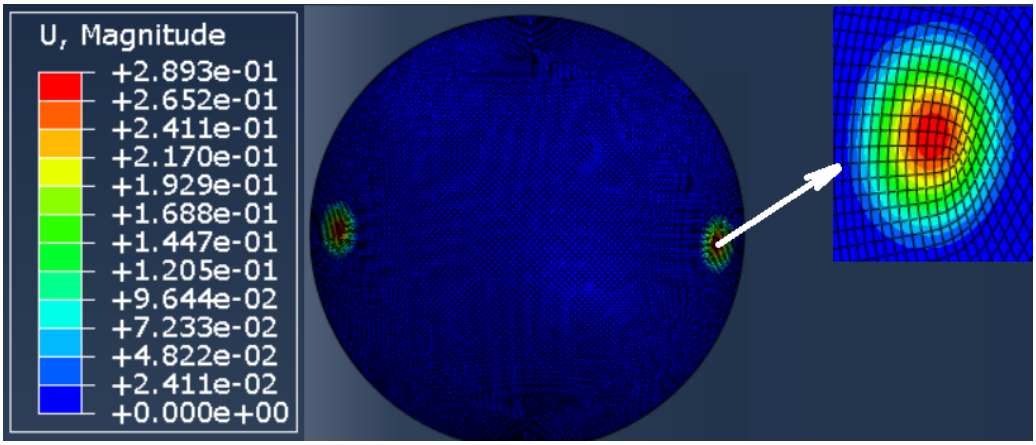


Fig. 4. Deformed shape of EPS with maximum displacements after GNA analysis without imperfection

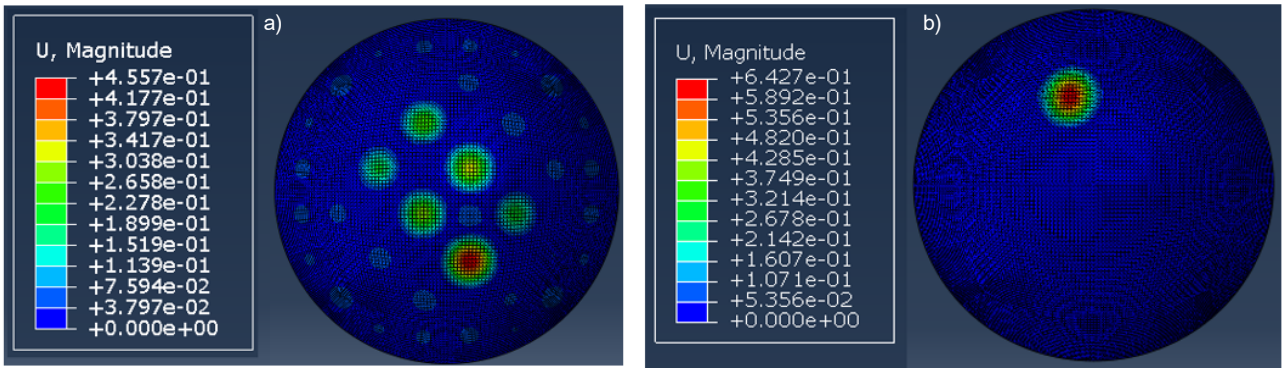


Fig. 5. Deformed shape with maximum displacements after GNA analysis with imperfection: a) concrete b) EPS

comparative displacement results demonstrate that the values are lower when computed numerically using software. This can be justified by the fact that numerical software analyses consider nonlinearity and plasticity effects, resulting in deflections that continue to decrease.

**Conclusion**

The results of the comparative analyses show that the maximum displacements from the LBA analyses are slightly higher than those from the GNA. It is known that in a spherical shell buckling case, snap-through buckling controls the behavior, and the difference in the results of these two analyses identifies an elastic imperfection reduction value derived from this snap-through buckling. The real buckling strength of a perfect shell is detected more accurately by GNA than by LBA. This is due to the fact that GNA follows a progressive alteration of

Table 2. **Loading displacements of concrete and EPS shells**

| **Concrete ($E_c$ = 30 GPA; v = 0.2; $\gamma_c$ = 24 kN/m³)** | | | | **EPS ($E_{eps}$ = 1.32 GPA; v = 0.27; $\gamma_c$ = 0.24 kN/m³)** | | | |
|---|---|---|---|---|---|---|---|
| t, thickness (m) | $q_{(self\text{-}weight)}$ (N/m²) | $q_{(DL+LL)}$ (N/m²) | Displacement (mm) | t, thickness (m) | $q_{(self\text{-}weight)}$ (N/m²) | $q_{(DL+LL)}$ (N/m²) | Displacement (mm) |
| 0.1 | 2880 | 5280 | 1.45 | 0.1 | 28.8 | 2428.8 | 15.64 |
| 0.15 | 4320 | 6720 | 1.23 | 0.15 | 43.2 | 2443.2 | 10.49 |
| 0.2 | 5760 | 8160 | 1.12 | 0.2 | 57.6 | 2457.6 | 7.91 |
| 0.25 | 7200 | 9600 | 1.06 | 0.25 | 72 | 2472 | 6.37 |
| 0.3 | 8640 | 11,040 | 1.01 | 0.3 | 86.4 | 2486.4 | 5.34 |

Table 3. **Loading displacements of concrete using analytical and numerical computation**

| **Concrete ($E_c$ = 30 GPA; v = 0.2; $\gamma_c$ = 24 kN/m³)** | | | **Analytical (manual)** | **Numerical (Abaqus)** |
|---|---|---|---|---|
| t, thickness (m) | $q_{(self\text{-}weight)}$ (N/m²) | $q_{(DL+LL)}$ (N/m²) | Displacement (mm) | Displacement (mm) |
| 0.1 | 2880 | 5280 | 1.45 | 1.78 |
| 0.15 | 4320 | 6720 | 1.23 | 1.08 |
| 0.2 | 5760 | 8160 | 1.12 | 0.82 |
| 0.25 | 7200 | 9600 | 1.06 | 0.69 |
| 0.3 | 8640 | 11,040 | 1.01 | 0.62 |

Table 4. **Loading displacements of EPS using analytical and numerical computation**

| **EPS ($E_{eps}$ = 1.32 GPA; v = 0.27; $\gamma_c$ = 0.24 kN/m³)** | | | **Analytical (manual)** | **Numerical (Abaqus)** |
|---|---|---|---|---|
| t, thickness (m) | $q_{(self\text{-}weight)}$ (N/m²) | $q_{(DL+LL)}$ (N/m²) | Displacement (mm) | Displacement (mm) |
| 0.1 | 28.8 | 2428.8 | 15.64 | 21.3 |
| 0.15 | 43.2 | 2443.2 | 10.49 | 8.76 |
| 0.2 | 57.6 | 2457.6 | 7.91 | 5.35 |
| 0.25 | 72 | 2472 | 6.37 | 3.82 |
| 0.3 | 86.4 | 2486.4 | 5.34 | 2.97 |

geometry under the applied loads resulting from the snap-through analysis. Moreover, the magnitudes of the maximum displacements from the nonlinear buckling analyses are significantly affected by the imperfections considered. The maximum displacement without imperfections, which was 90 mm for the concrete dome and 289 mm for the EPS dome, increased to 456 mm and 643 mm, respectively, when an imperfection factor of 0.055 was induced. This 4.5 times change in concrete and 2.22 times change in EPS corresponds to the fact that EPS has higher elasticity and Poisson's ratio compared to concrete.

Furthermore, to investigate the possibility of constructing domes using light-weight EPS material, the same geometric model was subjected to a factored ultimate load comprising self-weight and a live load of 1.5 kN/m². The total load imposed was 2428.8 N/m², which is 2.3 times less than the maximum buckling pressure of 5560 N/m². This total loading was found to produce a maximum displacement of 15.64 mm for the spherical shell with a thickness of 100 mm and a radius of 30 m. Although the displacement values are found to be very small and feasible for real-world construction, the actual ultimate loading, which is close to its buckling pressure, can be questioned, especially compared to that of concrete. In the case of concrete, the ultimate loading is 5280 N/m², which is 23 times less than the maximum buckling pressure of 122,364 N/m². To achieve more reliable buckling factors, the geometry of the EPS model was modified to a thickness of 200 mm. With an LBA eigenvalue of 71,190 N/m², the GNA (with imperfection) yields a maximum buckling pressure of 37,322 N/m², indicating a more accurate assessment. This thickness, loaded with a factored ultimate load of 2429 N/m², exhibits a maximum deflection of 15.4 mm.

Finally, the paper recommends conducting a practical large-scale experiment on EPS domes. Further research should investigate methods for constructing curved surface EPS domes using innovations such as cast in-situ techniques and/or robotic arm technologies.

**Acknowledgements**

This publication has been supported by the RUDN University Scientific Projects Grant System, project No. 202247-2-000.

**References**

Adriaenssens, S., Block, P., Veenendaal, D., and Williams, C. (2014). *Shell structures for architecture: form finding and optimization*. London and New York: Routledge Taylor & Francis Group, 323 p.

Bushnell, D. (1981). Buckling of shells—pitfall for designers. *AIAA Journal*, Vol. 19, No. 9, pp. 1183–1226. DOI: 10.2514/3.60058.

Eisenbach, P. (2017). *Processing of slender concrete shells — fabrication and installation*. [online] Available at: http://www.uni-kassel.de/upress/online/OpenAccess/978-3-7376-0258-7.OpenAccess.pdf [Date accessed April 18, 2021].

Ellobody, E., Feng, R., and Young, B. (2014). Chapter 4 - Linear and non-linear finite element analyses. In: Ellobody, E., Feng, R., and Young, B. (eds.). *Finite Element Analysis and Design of Metal Structures*. Waltham: Butterworth-Heinemann, pp. 56–71. DOI: 10.1016/B978-0-12-416561-8.00004-4.

Farshad, M. (1992). *Design and analysis of shell structures*. Dordrecht: Springer-Science+Business Media, 424 p. DOI: 10.1007/978-94-017-1227-9.

Gagg, C. R. (2014). Cement and concrete as an engineering material: An historic appraisal and case study analysis. *Engineering Failure Analysis*, Vol. 40, pp. 114–140. DOI: 10.1016/j.engfailanal.2014.02.004.

Huijben, F., van Herwijnen, F., and Nijsse, R. (2011). *Concrete shell structures revisited: introducing a new and 'low-tech' construction method using vacuumatics formwork*. [online] Available at: http://resolver.tudelft.nl/uuid:18354f6f-2187-467f-ad98-bc815caa285b [Date accessed January 10, 2023].

Hutchinson, J. W. and Thompson, J. M. T. (2017). Nonlinear buckling behaviour of spherical shells: barriers and symmetry-breaking dimples. *Philosophical Transactions of the Royal Society A*, Vol. 375, Issue 2093, 20160154. DOI: 10.1098/rsta.2016.0154.

Ibrahim, D., Bankole, O. C., Ma'aji, S. A., Ohize, E. J., and Abdul, B. K. (2013). Assessment of the strength properties of polystyrene material used in building construction in Mbora district of Abuja, Nigeria. *International Journal of Engineering Research and Development*, Vol. 6, Issue 12, pp. 80–84.

Imran, M., Shi, D., Tong, L., Waqas, H. M., Muhammad, R., Uddin, M., and Khan, A. (2020). Design optimization and non-linear buckling analysis of spherical composite submersible pressure hull. *Materials*, Vol. 13, Issue 11, 2439. DOI: 10.3390/ma13112439.

Jovanovic, M., Vucic, M., Mitov, D., Tepavčević, B., Stojakovic, V., and Bajsanski, I. (2017). Case specific robotic fabrication of foam shell structures. *Fabrication - Robotics*, Vol. 2, pp. 135–142.

Khalaj, O., Azizian, M., Tafreshi, S. N. M., and Mašek, B. (2017). Laboratory investigation of buried pipes using geogrid and EPS geofoam block. *IOP Conference Series: Earth and Environmental Science*, Vol. 95, Issue 2, 022002. DOI: 10.1088/1755-1315/95/2/022002.

Khalaj, O., Siabil, S. M. A. G., Tafreshi, S. N. M., Kepka, M., Kavalir, T., Křížek, M., and Jeníček, S. (2020). The experimental investigation of behaviour of expanded polystyrene (EPS). *IOP Conference Series: Materials Science and Engineering*, Vol. 723, 012014. DOI: 10.1088/1757-899X/723/1/012014.

LUSAS (2017). CSN/LUSAS/1014. *Non-linear buckling analysis with initial imperfection. Customer support note*. [online] Available at: https://www.lusas.com/user_area/documentation/1014_Nonlinear%20Buckling%20Analysis%20with%20Initial%20Imperfection.pdf [Date accessed January 10, 2023].

Mekjavić, I. (2011). Buckling analysis of concrete spherical shells. *Tehnički vjesnik*, Vol. 18, No. 4, pp. 633–639. DOI: 10.17265/1934-7359/2012.07.013.

Ni, X., Wu, Z., Zhang, W., Lu, K., Ding, Y., and Mao, S. (2020). Energy utilization of building insulation waste expanded polystyrene: pyrolysis kinetic estimation by a new comprehensive method. *Polymers*, Vol. 12, Issue 8, 1744. DOI: 10.3390/polym12081744.

Novoselac, S., Ergić, T., and Baličević, P. (2012). Linear and nonlinear buckling and post buckling analysis of a bar with the influence of imperfections. *Tehnički vjesnik*, Vol. 19, No. 3, pp. 695–701.

Ramli Sulong, N. H., Mustapa, S. A. S., and Abdul Rashid, M. K. (2019). Application of expanded polystyrene (EPS) in buildings and constructions: A review. *Journal of Applied Polymer Science*, Vol. 136, Issue 20, 47529. DOI: 10.1002/app.47529.

Saheed, S., Aziz, F. N. A. A., Amran, M., Vatin, N., Fediuk, R., Ozbakkaloglu, T., Murali, G., and Mosaberpanah, M. A. (2020). Structural performance of shear loaded precast EPS-foam concrete half-shaped slabs. *Sustainability*, Vol. 12, Issue 22, 9679. DOI: 10.3390/su12229679.

Semenov, A. A. (2016). Strength and stability of geometrically nonlinear orthotropic shell structures. *Thin-Walled Structures*, Vol. 106, pp. 428–436. DOI: 10.1016/j.tws.2016.05.018.

Ter Maten, R. N., Grunewald, S., and Walraven, J.C. (2013). UHPFRC in large span shell structures. In: *Proceedings of the RILEM-fib-AFGC international symposium on ultra-high performance fibre-reinforced concrete*, October 1–3, 2013, Marseille, France, pp. 327–334.

Tomas, A., Marti, P., and Tovar, J. P. (2009). Imperfection sensitivity in the buckling of single curvature concrete shells. In: *Proceedings of the International Association for Shell and Spatial Structures (IASS) Symposium 2009*, 28 September – 2 October, 2009, Valencia, Spain, pp. 1713–1721.

Vilau, C. and Dudescu, M. C. (2020). Investigation of mechanical behaviour of expanded polystyrene under compressive and bending loadings. *Materiale Plastice*, Vol. 57, Issue 2, pp. 199–207. DOI: 10.37358/MP.20.2.5366.

Wagner, H. N. R., Hühne, C., Zhang, J., and Tang, W. (2020). On the imperfection sensitivity and design of spherical domes under external pressure. *International Journal of Pressure Vessels and Piping,* Vol. 179, 104015. DOI: 10.1016/j.ijpvp.2019.104015.

# СРАВНИТЕЛЬНЫЙ АНАЛИЗ ПОТЕРИ УСТОЙЧИВОСТИ БЕТОННЫХ И ПЕНОПОЛИСТИРОЛЬНЫХ КУПОЛЬНЫХ ОБОЛОЧЕК

Хабте Йоханнес Дамир[1,2]*, Марина Рынковская[1], Иссайас Андей Сереке[1,2]

[1] Российский университет дружбы народов имени Патриса Лумумбы (РУДН), Москва, Россия
[2] Инженерно-технологический колледж Майнефхи, Асмэра, Эритрея

*E-mail: habte88eng@gmail.com

**Аннотация**:
**Введение:** Известны исследования анализа поведения бетонных сферических оболочек при потере устойчивости. Тем не менее, отсутствуют исследования, изучающие поведение оболочек из пенополистирола при потере устойчивости. Пенополистирол характеризуется довольно низким собственным весом по сравнению с бетоном. **Цель данной работы** — исследование сравнительных характеристик потери устойчивости бетонных оболочек и оболочек из пенополистирола. Были приняты во внимание собственный вес и временная нагрузка 1,5 кН/м$^2$. **Методы:** С помощью программного обеспечения Abaqus выполнены линейный расчет устойчивости (LBA) и геометрически нелинейный расчет устойчивости (GNA) образцов куполов с учетом несовершенств формы и без их учета. Сравнительный анализ показал, что критическое давление потери устойчивости сферических оболочек из пенополистирола и бетона одинаковой геометрии составило 122 634 Н/м$^2$ и 5560 Н/м$^2$ соответственно. Отношение критического давления потери устойчивости к практической предельной нагрузке (постоянная нагрузка + временная нагрузка) составило 23,2 для бетона и 2,22 для пенополистирола. Более того, увеличение толщины пенополистирола со 100 до 200 мм увеличило коэффициент критической нагрузки при потере устойчивости в 15,4 раза. Максимальное смещение пенополистирола при нагрузке (15,6 мм) было в разы меньше смещения при потере устойчивости. **Этот результат** демонстрирует возможность изготовления оболочек из пенополистирола, при этом необходимо провести дальнейшие исследования по выбору оптимальной геометрии и механизма изготовления.

**Ключевые слова:** оболочки, потеря устойчивости, купол, бетон, пенополистирол.